

Influence of defects on the lattice constant of GaMnAsJ. Sadowski^{1,2} and J. Z. Domagala²¹MAX-Lab, Lund University, P.O. Box 118, SE-221 00 Lund, Sweden²Institute of Physics, Polish Academy of Sciences, Al. Lotników 32/46, PL-02-668 Warszawa, Poland

(Received 1 September 2003; revised manuscript received 4 November 2003; published 19 February 2004)

We study the influence of the major compensating defects As antisites and Mn interstitials known to occur in the GaMnAs ferromagnetic semiconductor on its structural properties. Our experimental results show that there is a balance between Mn interstitial and As antisite defects, leading to the reduced density of one type of defect upon increasing the density of the other defect. Significant differences in the lattice parameters of GaMnAs with different balances between these two types of defects were observed. The annealing-induced reduction of the GaMnAs lattice constant is inhibited in samples with a large density of As antisites.

DOI: 10.1103/PhysRevB.69.075206

PACS number(s): 71.55.Eq, 75.50.Pp

There has been considerable increase of research activity in ferromagnetic semiconductors (FMSs) in recent years. Although known for quite a long time, for example in EuS, EuO,¹ and IV-VI narrow gap materials alloyed with Mn (PbSnMnTe),² ferromagnetism in semiconductors has gained renewed interest due to the prospects of using these materials in magnetoelectronic (spintronic) devices. The advent of the III-V FMSs InMnAs (Ref. 3) and GaMnAs (Ref. 4) in 1992 and 1996, respectively, generated momentum in the research activity in this area, due to their compatibility with the existing III-V semiconductor technology. The extensive research activity in the field caused considerable progress in both understanding the physical phenomena^{5–10} leading to ferromagnetism in III-V FMSs and improving the magnetotransport properties of these materials.^{11–15} This very recently led to an increase of T_c from the previously established limit⁴ of 110 K to 160–170 K.^{11,12,16} Different theoretical approaches to FMSs foresee considerably higher T_c ,^{5–10} so further progress in that direction cannot be excluded. The recent advancements in increasing T_c in GaMnAs were possible due to recognizing the most important defects compensating the Mn acceptors. However, in contrast to previous studies,^{17–19} where only As antisites (As_{Ga}) were considered, nowadays only Mn interstitial defects (Mn_i), recently verified experimentally to occur in GaMnAs,²⁰ are taken into account.²¹ On the other hand, it is obvious that both Mn_i and As_{Ga} are present in GaMnAs. Moreover, concentrations of these two defects are expected to be close to each other, 0.1–1% (or even 1.75% as suggested by some theoretical work¹⁹) for As_{Ga} and up to 2% for Mn_i .²² As shown by several groups,^{20,23–26} control over Mn_i defects is possible via the postgrowth annealing procedures. It was demonstrated²⁰ that postgrowth annealing reduces the concentration of Mn_i defects in the bulk of the GaMnAs layers, although it is not clear what happens to the Mn atoms removed from the interstitial positions. There are some suggestions that they segregate at the GaMnAs surface.^{27,28}

As reported by Yu *et al.*,²⁰ it is possible to detect Mn_i atoms directly, by particle-induced x-ray emission and Rutherford backscattering methods. As concerns As antisites in GaMnAs, no experimental data revealing their concentrations are available yet. On the other hand, the As antisite defects in GaAs grown by low-temperature (LT) molecular

beam epitaxy (MBE) have already been investigated in detail,^{29–31} and it is well known how to estimate their content. Typical methods used for evaluation of As_{Ga} in LT GaAs, namely, lattice constant and optical absorption/emission measurements, are difficult in the case of GaMnAs. The use of optical methods is complicated due to the very poor optical quality of this compound. Straightforward information on As_{Ga} concentration from lattice constant measurements is hard to obtain since the GaMnAs lattice expansion is due to several factors, such as Mn at Ga sites, Mn at interstitial sites, As at Ga sites,³² and other defects typical for LT GaAs. As is well known,^{29,30} the density of As antisites in LT GaAs ($[\text{As}_{\text{Ga}}]$) depends on the MBE growth conditions and can be adjusted by varying either the substrate temperature (T_s) or the As to Ga flux ratio. Increasing T_s decreases $[\text{As}_{\text{Ga}}]$, whereas increasing As/Ga increases $[\text{As}_{\text{Ga}}]$.³⁰ In this work we used the latter way to change $[\text{As}_{\text{Ga}}]$ in both the LT GaAs buffers and the subsequently grown GaMnAs layers. We separate the influence of Mn_i and As_{Ga} defects on the lattice parameter a_{GaMnAs} by careful x-ray diffraction (XRD) measurements of $\text{Ga}_{0.96}\text{Mn}_{0.04}\text{As}$ samples, differing in the concentration of As antisites.

We investigated three sets of $\text{Ga}_{0.96}\text{Mn}_{0.04}\text{As}$ layers grown on LT GaAs buffer layers, and a sequence of GaMnAs layers with Mn content increasing from 0.1% to 3.5%. The samples were grown in the Kryovak MBE system dedicated to III-Mn-V magnetic semiconductors. A valved cracker source was used to generate As_2 flux. Before the growth of $\text{Ga}_{0.96}\text{Mn}_{0.04}\text{As}$ layers, the LT GaAs buffers were deposited at the same substrate temperature (230 °C) and growth rate [0.2 monolayers (ML)/s] as further used for GaMnAs. Each of these samples was grown at a different As_2/Ga flux ratio and the other parameters like T_s and Mn content were the same. Samples 1, 2, and 3 were grown at As_2 to Ga flux ratios of 2, 5, and 9, respectively. The Mn content was set by the temperature of the Mn effusion cell, $T_{\text{Mn}} = 775$ °C, the same for all three samples, and verified by measuring the differences in the growth rates between GaMnAs and LT GaAs using reflection high-energy electron diffraction intensity oscillations.³³ After MBE growth the substrate temperature was decreased rapidly, and the samples were taken out of the vacuum system and cleaved into four pieces. One piece was left unchanged; the other pieces were placed on

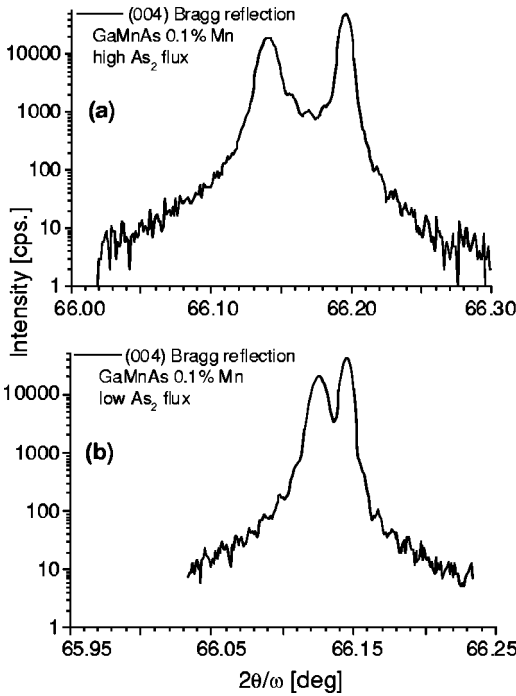


FIG. 1. (004) x-ray Bragg reflections for two $\text{Ga}_{0.999}\text{Mn}_{0.001}\text{As}$ layers grown at (a) high and (b) low excess As_2 flux. Peak on the right side, reflection from the $\text{GaAs}(001)$ substrate; peak on the left side, reflection from the GaMnAs layer

the molybdenum holder again, put into the vacuum system, and transferred to the MBE growth chamber for annealing at high vacuum. The annealings were performed in such a way that in each annealing run the pieces of all three samples were annealed together. Annealings at different temperatures were done for different pieces of each sample. The annealing temperatures were chosen to be 240, 260, and 280 °C; the annealing time was 2 h in each case.

For XRD measurements, we used a Philips X-pert high-resolution diffractometer with a collimating mirror. Samples were measured in two different configurations: double axis for ω and $\omega/2\theta$ scans; triple axis with an analyzer, for $2\theta/\omega$ scans and reciprocal space mapping. Both symmetrical and asymmetrical Bragg reflections were measured. Our investigations of the GaMnAs structure by XRD methods were inspired by the observation of significant influence of the growth conditions, namely, As to Ga flux ratio and substrate temperature, on the GaMnAs lattice constant. This is illustrated in Fig. 1. Two GaMnAs samples measured by XRD have the same Mn content of 0.1%, they were grown at the same substrate temperature (230 °C), and differ in the As_2 to Ga flux ratio, which is 9 for sample (a) and 2 for sample (b). A clear difference in the angular positions of the GaMnAs (004) diffraction peaks, reflecting differences between the lattice parameters of the two samples, can be seen. A similar effect occurs in GaMnAs with a higher Mn content. Our observations are consistent with the results published by other groups. Shott *et al.*³⁴ investigated the effect of the substrate temperature on the GaMnAs lattice parameter. The authors observed significant changes of the GaMnAs lattice constant for samples with the same Mn content grown at

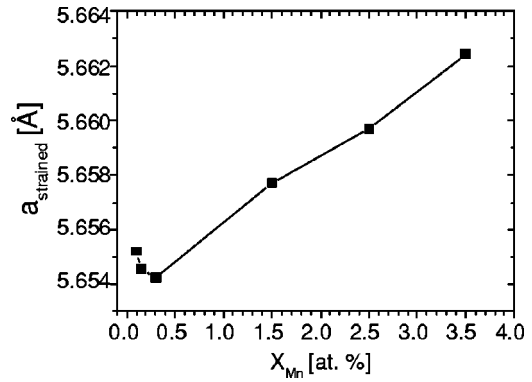


FIG. 2. Perpendicular (strained) lattice constant of $\text{Ga}_{1-x}\text{Mn}_x\text{As}$ with Mn content x from 0.1% to 3.5%. At $x = 0.3\%$, a_{strained} reaches the lowest value.

different T_s . These observations make it questionable to extrapolate the GaMnAs lattice constant to zinc blende MnAs or to estimate the Mn content in GaMnAs from lattice constant measurements.

Another interesting feature concerning the GaMnAs lattice parameter is illustrated in Fig. 2. This figure shows the dependence of the strained, perpendicular GaMnAs lattice constant on the Mn content, starting from diluted samples containing 0.1% Mn up to a Mn content (X_{Mn}) of 3.5%. It is interesting to notice that a_{GaMnAs} decreases with increasing X_{Mn} in the very low Mn concentration range. For Mn composition increasing from 0.1% to 0.3%, a_{GaMnAs} decreases, reaches a minimum value at about 0.3% Mn, and then increases proportionally to X_{Mn} . This decrease of the GaMnAs lattice constant in the much diluted Mn concentration limit was not reported before, to our best knowledge. It is discussed later in the paper.

Figure 3 shows the XRD results for three $\text{Ga}_{0.96}\text{Mn}_{0.04}\text{As}$ layers grown on thick LT GaAs buffers. The most interesting aspects of Fig. 3 are the dependences of the angular positions of the (006) Bragg reflections of LT GaAs buffers and GaMnAs layers on the As_2/Ga flux ratio ($r_{\text{As}_2/\text{Ga}}$). These Bragg reflections are a measure of the perpendicular, strained lattice parameter of the epilayers. In sample 1 grown at

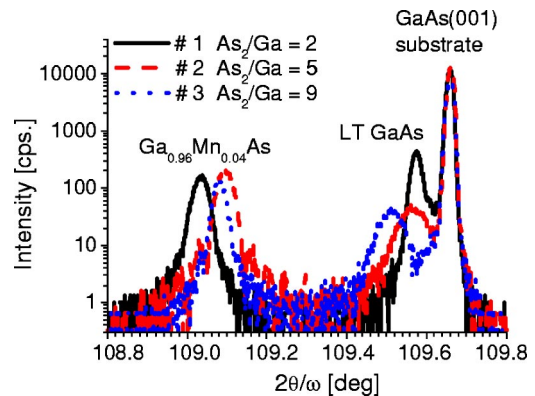


FIG. 3. (Color online) (006) x-ray Bragg reflections for three $\text{Ga}_{0.96}\text{Mn}_{0.04}\text{As}$ samples grown on LT GaAs buffers at different As_2/Ga flux ratios of 2, sample 1, solid line; 5, sample 2, dashed line; 9, sample 3, dotted line.

TABLE I. Parameters of as-grown, nonannealed $\text{Ga}_{0.96}\text{Mn}_{0.04}\text{As}$ samples and LT GaAs buffer layers.

Sample No.	LT GaAs thickness (μm)	GaMnAs thickness (μm)	LT GaAs		$[\text{As}_{\text{Ga}}]$	$[\text{Mn}_{\text{I}}]$
			a_{strained} a_{relaxed} (\AA)	a_{strained} a_{relaxed} (\AA)		
1	0.80	0.50	5.6564	5.67530	0.20%	0.82%
			5.6549	5.66408		
			5.65688	5.67316		
2	0.20	0.30	5.6551	5.66305	0.23%	0.70%
			5.6587	5.67358		
3	0.20	0.40	5.6560	5.66325	0.35%	0.64%

$r_{\text{As/Ga}}=2$ the relaxed lattice constant of the LT GaAs buffer (calculated from the measured strained lattice parameter) is the lowest of all three samples: $a_{\text{LT GaAs}}(1)=5.6549 \text{ \AA}$, whereas the lattice constant of GaMnAs, a_{GaMnAs} , is the highest. In samples 2 and 3 grown at medium and high $r_{\text{As/Ga}}$, respectively, $a_{\text{LT GaAs}}$ increases with increasing $r_{\text{As/Ga}}$, but a_{GaMnAs} changes slightly in the opposite way to $a_{\text{LT GaAs}}$, i.e., it is largest for sample 1, and smaller for samples 2 and 3.

As reported by many groups, the changes in the LT GaAs lattice constant are caused by the different densities of As antisites. Following the relation between $a_{\text{LT GaAs}}$ and the density of As_{Ga} defects given by Liu *et al.*,²⁹ we estimated $[\text{As}_{\text{Ga}}]$ to be 0.20%, 0.23%, and 0.35% for samples 1, 2, and 3, respectively. Assuming that $[\text{As}_{\text{Ga}}]$ in GaMnAs is the same as in LT GaAs buffers grown prior to the GaMnAs deposition and knowing a_{GaMnAs} from measurements, we can estimate the contribution of Mn interstitial defects to a_{GaMnAs} . We are using the results of the theoretical approach of Masek *et al.*,³² who calculated the dependence of a_{GaMnAs} on $[\text{As}_{\text{Ga}}]$, $[\text{Mn}_{\text{I}}]$, and Mn at Ga sites to follow the formula

$$a_{\text{GaMnAs}}(x,y,z) = a_0 + 0.02x + 0.69y + 1.05z, \quad (1)$$

where a_0 is the lattice constant of GaAs without defects, x is the concentration of Mn at Ga sites, y is the concentration of As antisites, and z is the concentration of Mn at interstitial sites.

Using the values of $[\text{As}_{\text{Ga}}]$ calculated from the lattice parameters of LT GaAs buffers and the measured values of a_{GaMnAs} for samples 1, 2, and 3, we obtain the following concentrations of Mn_{I} [z in Eq. (1)]:

$$\text{sample 1: } [\text{Mn}_{\text{I}}]=0.82\% \quad \text{for } [\text{As}_{\text{Ga}}]=0.20\%,$$

$$\text{sample 2: } [\text{Mn}_{\text{I}}]=0.70\% \quad \text{for } [\text{As}_{\text{Ga}}]=0.23\%,$$

$$\text{sample 3: } [\text{Mn}_{\text{I}}]=0.64\% \quad \text{for } [\text{As}_{\text{Ga}}]=0.35\%.$$

The numerical parameters obtained from the results of XRD measurements shown in Fig. 3 and used for calculations of $[\text{Mn}_{\text{I}}]$ from formula (1) are given in Table I.

Assuming that the a_{GaMnAs} dependence on x,y,z follows Eq. (1), we can explain the decrease of a_{GaMnAs} at low Mn content region, shown in Fig. 2. If Mn atoms are introduced into the LT GaAs lattice in a very small amount (below 0.3%

in our case), they enter only the Ga sites. Since the concentration of As_{Ga} is higher than the Mn content, the system does not need any additional compensating defects other than As antisites to overcompensate the Mn acceptors. Increasing the Mn content up to the $[\text{As}_{\text{Ga}}]$ value (0.1–0.5% depending on the LT MBE growth conditions) finally leads to the situation when the concentration of Mn acceptors is higher than the concentration of As antisite donors and another kind of defect is necessary to compensate the Mn acceptors. These defects may be Mn at interstitial positions. Following the formula (1), in the low-Mn-concentration limit and below the compensation point, we expect $[\text{As}_{\text{Ga}}]$ to be constant and $[\text{Mn}_{\text{I}}]$ to be equal to zero. This gives an increase of the lattice constant of 0.00002 \AA for GaMnAs containing 0.1% Mn. This is below the resolution of a typical XRD setup. That means that Mn should not influence the measured value of the GaMnAs lattice constant in the case when all the Mn atoms are situated at the Ga sites, in this low-Mn-content range. The slight decrease of a_{GaMnAs} with increasing X_{Mn} at $0.1\% < X_{\text{Mn}} < 0.3\%$ can be caused by lattice contraction due to the ionization of deep As_{Ga} donors by Mn acceptors. Similar effects were observed by Specht *et al.*³⁵ in LT GaAs doped to p type by Be and C. The authors observed ionization of As antisites proportional to the concentration of p -type dopants and concluded that ionized As_{Ga} defects have different (smaller) sizes than neutral As_{Ga} . Attributing the $a_{\text{GaMnAs}}(X_{\text{Mn}})$ lattice constant minimum to 100% ionization of As_{Ga} donors by Mn acceptors, we may conclude that the concentration of As_{Ga} is equal to 0.15% at the 100% compensation point. It is half of X_{Mn} since As_{Ga} is a double donor.

In order to verify the estimation of Mn interstitial concentrations in GaMnAs with different concentrations of As antisites, we used a procedure that is recognized to remove Mn_{I} defects (but does not affect As_{Ga}), namely, the low-temperature postgrowth annealing.²⁰ Figure 4 shows the annealing effects on both LT GaAs buffers and GaMnAs layers of samples 1, 2, and 3. As seen in Figs. 4(a), 4(b), and 4(c), the effect of annealing on the lattice constant of the LT GaAs layers is negligible. The LT GaAs lattice parameter scarcely changes at all even after the highest-temperature annealing. That means that the defects present in LT GaAs are not affected by annealing to 280°C and below. This is consistent with the literature reports³⁵ indicating that LT GaAs changes

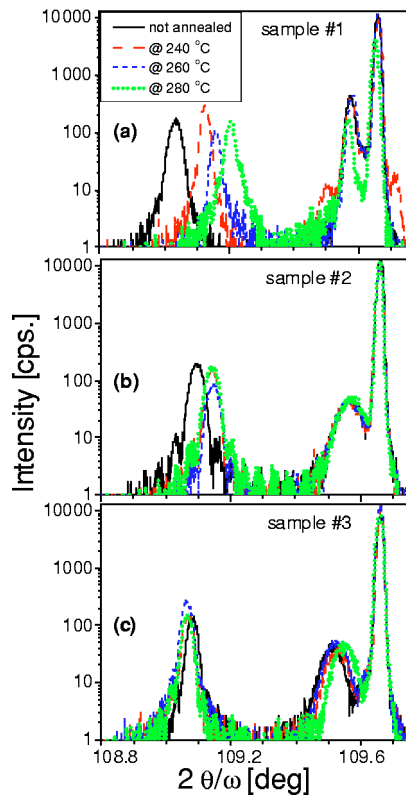


FIG. 4. (Color online) (006) x-ray Bragg reflections for samples 1(a), 2(b), and 3(c) before and after postgrowth annealing. Solid, dashed, short-dashed, and dotted lines correspond to the samples nonannealed and annealed at 240, 260, and 280 °C, respectively.

its defect structure upon annealing to much higher temperatures—above 400 °C. In the case of GaMnAs layers, the influence of annealing on a_{GaMnAs} is significant. The most interesting effect is the decrease of annealing-induced changes in a_{GaMnAs} with increasing value of the excess As flux used during GaMnAs LT MBE growth. For sample 3, grown at the highest $r_{\text{As/Ga}}$ a slight increase of a_{GaMnAs} after annealing was observed. This is in contrast to what is observed for samples 1 and 2, and to the observations reported

by other groups,^{36,37} which all show decreased lattice constant upon annealing. The annealing-induced decrease of the GaMnAs lattice constant can be interpreted as an effect of removing Mn from interstitial sites. This was suggested theoretically³² and recently shown experimentally.³⁷ Our results showing the disappearance of this effect for samples with a high density of As antisites suggest that increasing density of As antisites in GaMnAs is accompanied by a decreasing density of Mn interstitials. A simple analysis of the influence of Mn interstitials and As antisites on the GaMnAs lattice parameter based on the results of theoretical model by Masek *et al.*³² confirms this conclusion. This is also in agreement with the recent theoretical work of Mahadevan and Zunger,³⁸ who found that the MBE growth of GaMnAs at high excess As conditions inhibits formation of Mn_i defects. However, As-rich growth conditions promote the formation of As antisites, which are efficient compensating centers that cannot be removed by postgrowth annealing, in contrast to the Mn interstitials.

In summary, we have shown that the lattice constant of GaMnAs depends on the concentration of both As antisite and Mn interstitial defects. At very low Mn concentrations, the GaMnAs lattice constant slightly decreases with increasing Mn content, up to the Mn content at which As antisite donors are fully compensated by Mn acceptors. Further increase of Mn concentration leads to an increase of a_{GaMnAs} , due to the manganese at gallium sites and the increased density of manganese at interstitial sites. Lattice constant measurements of GaMnAs with different concentrations of As antisites as well as the results of low-temperature annealing experiments indicate that there is a balance between Mn interstitials and As antisite defects during the low-temperature MBE growth process of GaMnAs. This leads to the reduced density of one type of defect upon increased density of the other defect in as-grown GaMnAs films.

The authors would like to thank Dr. Janusz Kanski from Chalmers University of Technology, Göteborg, Sweden for valuable discussions. This work was supported in part by the European Commission program ICA1-CT-2000-70018 (Centre of Excellence CELDIS).

¹L. Passell, O. W. Dietrich, and J. Als-Nielsen, *Phys. Rev. B* **14**, 4897 (1976).

²T. Story, R. R. Gałazka, R. B. Frankel, and P. A. Wolff, *Phys. Rev. Lett.* **56**, 777 (1986).

³H. Ohno, H. MuneKata, T. Penney, S. von Molnar, and L. L. Chang, *Phys. Rev. Lett.* **68**, 2664 (1992).

⁴H. Ohno, A. Shen, F. Matsukura, A. Oiwa, A. Endo, S. Katsumoto, and Y. Iye, *Appl. Phys. Lett.* **69**, 363 (1996).

⁵T. Dietl, H. Ohno, F. Matsukura, J. Cibert, and D. Ferrand, *Science* **287**, 1019 (2000).

⁶T. Dietl, F. Matsukura, and H. Ohno, *Phys. Rev. B* **66**, 033203 (2002).

⁷A. Kaminski and S. Das Sarma, *Phys. Rev. Lett.* **88**, 247202 (2002).

⁸T. Jungwirth, Jürgen König, Jairo Sinova, J. Kucera, and A. H.

MacDonald, *Phys. Rev. B* **66**, 012402 (2002).

⁹Malcolm P. Kennett, Mona Berciu, and R. N. Bhatt, *Phys. Rev. B* **66**, 045207 (2002).

¹⁰L. Bergqvist, P. A. Korzhavyi, B. Sanyal, S. Mirbt, I. A. Abrikosov, L. Nordström, E. A. Smirnova, P. Mohn, P. Svedlindh, and O. Eriksson, *Phys. Rev. B* **67**, 205201 (2003).

¹¹K. W. Edmonds, K. Y. Wang, R. P. Campion, A. C. Neumann, N. R. S. Farley, B. L. Gallagher, and C. T. Foxon, *Appl. Phys. Lett.* **81**, 4991 (2002).

¹²K. C. Ku, S. J. Potashnik, R. F. Wang, S. H. Chun, P. Schiffer, N. Samarth, M. J. Seong, A. Mascarenhas, E. Johnston-Halperin, R. C. Myers, A. C. Gossard, and D. D. Awschalom, *Appl. Phys. Lett.* **82**, 2302 (2003).

¹³R. Mathieu, B. S. Sørensen, J. Sadowski, U. Södervall, J. Kanski,

- P. Svedlindh, P. E. Lindelof, D. Hrabovsky, E. Vanelle, *Phys. Rev. B* **68**, 205210 (2003).
- ¹⁴D. Chiba, K. Takamura, F. Matsukura, and H. Ohno, *Appl. Phys. Lett.* **82**, 3020 (2003).
- ¹⁵I. Kuryliszyn, T. Wojtowicz, X. Liu, J. K. Furdyna, W. Dobrowolski, J. M. Broto, O. Portugall, H. Rakoto, and B. Raquet, *J. Supercond.* **16**, 63 (2003).
- ¹⁶Ahsan M. Nazmul, S. Sugahara, and M. Tanaka, *Phys. Rev. B* **67**, 241308 (2003).
- ¹⁷S. J. Potashnik, K. C. Ku, S. J. Potashnik, K. C. Ku, S. H. Chun, J. J. Berry, N. Samarth, and P. Schiffer, *Appl. Phys. Lett.* **79**, 1495 (2001).
- ¹⁸S. Sanvito and N. A. Hill, *Appl. Phys. Lett.* **78**, 3493 (2001).
- ¹⁹P. A. Khorzhavyi, I. A. Abrikosov, E. A. Smirnova, L. Bergqvist, P. Mohn, R. Mathieu, P. Svedlindh, J. Sadowski, E. I. Isaev, Yu. Kh. Vekilov, and O. Eriksson, *Phys. Rev. Lett.* **88**, 187202 (2002).
- ²⁰K. M. Yu, W. Walukiewicz, T. Wojtowicz, I. Kuryliszyn, X. Liu, Y. Sasaki, and J. K. Furdyna, *Phys. Rev. B* **65**, 201303 (2002).
- ²¹J. Blinowski and P. Kacman, *Phys. Rev. B* **67**, 121204 (2003).
- ²²In the nonannealed GaMnAs samples, compensation of Mn acceptors is up to 70%. This can be reduced to 10% by postgrowth annealing. Since the annealing affects mainly Mn_I, then in the nonannealed samples the concentration of Mn interstitials is expected to be up to 30% of Mn_{Ga} concentration.
- ²³K. W. Edmonds, K. Y. Wang, R. P. Champion, A. C. Neumann, C. T. Foxon, B. L. Gallagher, and P. C. Main, *Appl. Phys. Lett.* **81**, 3010 (2002).
- ²⁴M. B. Stone, K. C. Ku, S. J. Potashnik, B. L. Shen, N. Samarth, and P. Schiffer, *Appl. Phys. Lett.* **83**, 4568 (2003).
- ²⁵W. Limmer, A. Koeder, S. Frank, M. Glunk, W. Schoch, V. Avrutin, K. Zuern, R. Sauer, and A. Waag, *cond-mat/0307102* (unpublished).
- ²⁶B. S. Sorensen, J. Sadowski, R. Mathieu, P. Svedlindh, and P. E. Lindelof, *Appl. Phys. Lett.* **82**, 2287 (2003).
- ²⁷S. C. Erwin, and A. G. Petukhov, *Phys. Rev. Lett.* **89**, 227201 (2002).
- ²⁸K. W. Edmonds, P. Boguslawski, B. L. Gallagher, R. P. Champion, K. Y. Wang, N. R. S. Farley, C. T. Foxon, M. Sawicki, T. Dietl, M. B. Nardelli, and J. Bernholc, *cond-mat/0307140* (unpublished).
- ²⁹X. Liu, A. Prasad, J. Nishio, E. R. Weber, Z. Liliental-Weber, and W. Walukiewicz, *Appl. Phys. Lett.* **67**, 279 (1995).
- ³⁰A. Suda and N. Otsuka, *Surf. Sci.* **458**, 162 (2000).
- ³¹T. E. M. Staab, R. M. Nieminen, J. Gebauer, R. Krause-Rehberg, M. Luysberg, M. Haugk, and Th. Frauenheim, *Phys. Rev. Lett.* **87**, 045504 (2001).
- ³²J. Masek, J. Kudrnovsky, and F. Maca, *Phys. Rev. B* **67**, 153203 (2003).
- ³³J. Sadowski, J. Z. Domagala, J. Bąk-Misiuk, S. Koleśnik, M. Sawicki, K. Świątek, J. Kanski, L. Ilver, and V. Ström, *J. Vac. Sci. Technol. B* **18**, 1697 (2000).
- ³⁴G. M. Schott, W. Faschinger, and L. W. Molenkamp, *Appl. Phys. Lett.* **79**, 1807 (2001).
- ³⁵P. Specht, R. C. Lutz, R. Zhao, E. R. Weber, W. K. Liu, K. Bacher, F. J. Towner, T. R. Stewart, and M. Luysberg, *J. Vac. Sci. Technol. B* **17**, 1200 (1999).
- ³⁶S. J. Potashnik, K. C. Ku, R. Mahendiran, S. H. Chun, R. F. Wang, N. Samarth, and P. Schiffer, *Phys. Rev. B* **66**, 012408 (2002).
- ³⁷I. Kuryliszyn-Kudelska, J. Z. Domagała, T. Wojtowicz, X. Liu, E. Lusakowska, W. Dobrowolski, and J. K. Furdyna, *cond-mat/0307467* (unpublished).
- ³⁸P. Mahadevan and A. Zunger, *Phys. Rev. B* **68**, 075202 (2003).